Li *et al. Soft Sci* 2023;3:22
DOI: 10.20517/ss.2023.11

Soft Science

Research Article

Open Access

Check for updates

Hair-compatible sponge electrodes integrated on VR headset for electroencephalography

Hongbian Li[1], Hyonyoung Shin[2], Minsu Zhang[2], Andrew Yu[1], Heeyong Huh[1], Gubeum Kwon[3], Nicholas Riveira[2], Sangjun Kim[4], Susmita Gangopadahyay[2], Jessie Peng[5], Zhengjie Li[1], Yifan Rao[1], Luis Sentis[1], José del R. Millán[2,6,7], Nanshu Lu[1,2,4,5,8,*]

[1]Department of Aerospace Engineering and Engineering Mechanics, The University of Texas at Austin, Austin, TX 78712, USA.
[2]Department of Electrical and Computer Engineering, The University of Texas at Austin, Austin, TX 78712, USA.
[3]Artue Associates Incorporated, Seoul, 04410, Republic of Korea.
[4]Department of Mechanical Engineering, The University of Texas at Austin, Austin, TX 78712, USA.
[5]Department of Biomedical Engineering, The University of Texas at Austin, Austin, TX 78712, USA.
[6]Department of Neurology, The University of Texas at Austin, Austin, TX 78712, USA.
[7]Mulva Clinic for the Neurosciences, The University of Texas at Austin, Austin, TX 78712, USA.
[8]Texas Materials Institute, The University of Texas at Austin, Austin, TX 78712, USA.

[*]**Correspondence to:** Prof. Nanshu Lu, Department of Aerospace Engineering and Engineering Mechanics, The University of Texas at Austin, 2617 Wichita St., Austin, TX 78712, USA. E-mail: nanshulu@utexas.edu

How to cite this article: Li H, Shin H, Zhang M, Yu A, Huh H, Kwon G, Riveira N, Kim S, Gangopadahyay S, Peng J, Li Z, Rao Y, Sentis L, Millán JdR, Lu N. Hair-compatible sponge electrodes integrated on VR headset for electroencephalography. *Soft Sci* 2023;3:22. https://dx.doi.org/10.20517/ss.2023.11

Received: 28 Feb 2023 **First Decision:** 4 Apr 2023 **Revised:** 9 May 2023 **Accepted:** 24 May 2023 **Published:** 3 Jul 2023

Academic Editors: Dae-Hyeong Kim, Zhifeng Ren **Copy Editor:** Lin He **Production Editor**: Dong-Li Li

Abstract

Virtual reality (VR) technology has emerged as a promising tool for brain-computer interaction and neuroscience research due to its ability to provide immersive and interactive experiences for its users. As a powerful tool to noninvasively monitor the cortex, electroencephalography (EEG) combined with VR represents an exciting opportunity for the measurement of brain activity during these experiences, providing insight into cognitive and neural processes. However, traditional gel-based EEG sensors are not compatible with VR headsets, and most emerging VR-EEG headsets utilizing rigid comb electrodes are uncomfortable after prolonged wear. To address this limitation, we created soft, porous, and hair-compatible sponge electrodes based on conductive poly(3,4-ethylenedioxythiophene) polystyrene sulfonate/melamine (PMA) and integrated them onto a VR headset through a customized, flexible circuit for multichannel EEG during VR task performing. Our PMA sponge electrodes can deform to make contact with the scalp skin through hairs under the pressure naturally applied by the strap of the VR headset. The specific contact impedance was consistently below 80 kΩ·cm^2, even at hairy sites. We demonstrated the capability of our VR-EEG headset by recording alpha rhythms during eye closure at both hairless

and hairy sites. In another demonstration, we developed a VR task to evoke the contingent negative variation potential and achieved a classification accuracy of 0.66 ± 0.07, represented by the cross-validated area under the receiver operating characteristic curve. Our sponge-electrode-integrated VR headset is user-friendly and easy to set up, marking a step toward future reliable, comfortable, and reusable VR-EEG technology.

Keywords: PEDOT:PSS, soft electrode, electroencephalography, virtual reality, brain-computer interface

INTRODUCTION

Electroencephalography (EEG) is a non-invasive technique that records neural activity from the scalp, offering high temporal resolution, affordability, and versatility[1-3] compared to alternative modalities such as functional magnetic resonance imaging (fMRI) and invasive electrocorticography (ECoG). EEG has been widely used for various applications, including sleep monitoring[4], clinical diagnosis and treatment of neurological disorders such as epilepsy[5] and stroke[6], and as a primary signal modality for both clinical and non-clinical brain-computer interfaces (BCI)[1,7-9]. In recent years, virtual reality (VR) technology has emerged as a new tool in the fields of cognition assessment[10], rehabilitation[11], pain relief[12], and BCI[13]. VR can create controlled environments that integrate intuitive, immersive, and interactive elements[14] with innovative input methods such as gaze direction and hand gestures, potentially replacing conventional visual stimulation and feedback techniques. Therefore, the integration of EEG and VR represents a promising opportunity for the improvement of both EEG and VR systems[15,16]. EEG can provide a real-time stream of brain activity and cognitive state information that can be utilized by the VR application, while VR can provide a unique environment for evoking and studying brain activity in realistic and immersive simulations.

Current EEG and VR systems are implemented separately in hardware, resulting in cumbersome and complicated systems when they are simply combined[16]. Emerging research has demonstrated the viability of integrating EEG electrodes directly on VR headsets for simultaneous EEG recording and VR stimulation[17,18], but these studies primarily target hairless areas such as the forehead. However, regions of interest for brain activity analysis and many BCI applications are often located underneath the hairy parts of the scalp such as the motor cortex and visual cortex, which are hard to access by existing VR-EEG systems. To overcome hair interference in conventional EEG, the conductive liquid gel is commonly used, but it is time-consuming to set up, limited in operating time, uncomfortable, and requires trained personnel[19]. Additionally, some ingredients in the gel electrodes, such as propylparaben, have been found to be harmful to the skin[20]. To address these issues, paintable gel electrodes with a fast liquid-to-solid transition speed have been developed, simplifying the scalp preparation and electrode application process and reducing the required time compared to commercial gel electrodes[21,22]. However, these electrodes require removal by washing off after use, limiting their integration with other systems for multiple uses.

Dry electrodes have gained attention for EEG due to their ease of use, setup, removal, and integration with wearable systems compared to gel electrodes[3]. Various dry electrode designs, including microneedle[23], nanotube[24], and pillar[25-27] electrodes, have been explored over the past decade. These electrodes can penetrate hair bundles to make direct contact with the scalp, providing reasonable EEG recordings. However, their fabrication processes are often complex microfabrication processes, which are high-cost and time-consuming[23,24]. Furthermore, transdermal microneedles can cause pain and potential skin infections[23,27]. Recent studies have found that soft electrodes made of elastomer pillars coated with conductive materials, such as gold[23] and poly(3,4-ethylenedioxythiophene) polystyrene sulfonate (PEDOT:PSS)[28], have greatly reduced stiffness and improved skin compatibility. However, an additional

adhesive layer is necessary to prevent the delamination of the coating layer under pillar deformation, which adds complexity and cost to the fabrication process.

Soft conductive sponges offer a hair-friendly option for EEG recording, as they can make better contact with the scalp when compressed despite hairs[29]. These sponge electrodes can be integrated onto various types of headwear such as caps[30] and headbands[31], making them ideal for portable and wireless EEG recording. Recent works reported that silver-nanowire-coated melamine (MA) sponges can record high-fidelity steady-state visual evoked potentials (SSVEP) on hairy scalps[29,32]. However, silver nanowires require a polymer coating for improved chemical stability and reduced toxicity. PEDOT:PSS is a conducting polymer with high chemical stability, conductivity, and biocompatibility[33,34]. It has both ionic and electronic conductivity, enabling lower contact impedance with the skin than that of gold[35]. These characteristics make PEDOT:PSS a popular choice for electrode materials in bioelectrical signal recording[9,28,35,36]. In this paper, we fabricate soft PEDOT:PSS/MA (PMA) sponge electrodes that can be easily integrated on a commercial VR headset for EEG recording during VR experiences. The PMA sponge electrode is mechanically compliant and can conform to the hairy scalp upon being pressed by the VR headset strap, resulting in high-fidelity multichannel EEG recordings. We developed a VR program to demonstrate the PMA sponge electrode-based VR-BCI system. We have successfully detected the contingent negative variation (CNV)-related potentials using our VR-EEG BCI system.

EXPERIMENTAL

Chemicals and materials

MA sponges were purchased from Amazon. PEDOT:PSS (Clevios PH1000, solid content 1.3%) was obtained from Heraeus Precious Metals North America Daychem LLC (Vandalia, OH, USA). Dimethyl sulfoxide (DMSO, 99.9%) was purchased from Beantown Chemical (Hudson, NH, USA). Copper films were purchased from Nimrod Copper Company. Solid gel electrodes (Kendall ECG electrodes) and comb electrodes were obtained from Kendall and OpenBCI (Brooklyn, NY, USA), respectively. All chemicals were used as received without further purification.

Fabrication of PMA sponges

PMA sponges were prepared by a dipping method. In brief, MA sponge pieces were punched into cylinders with a height of 10 mm and a diameter of 12 mm. A PEDOT:PSS solution was prepared by mixing 7 g of Clevios PH1000 dispersion and 3 g of DMSO under stirring at room temperature for 30 minutes. The MA sponge cylinders were then dipped into the PEDOT:PSS solution and squeezed four times to enhance infiltration of the PEDOT:PSS solution. The PEDOT:PSS solution with MA sponges was then placed into a desiccator and kept under vacuum for 15 minutes to further enhance infiltration of the PEDOT:PSS solution. The sponges were then scooped up, and excess PEDOT:PSS solution was removed using filter paper. The sponges were dried at 110 °C in an oven for 2 hours. After another dipping and drying process, PMA composite sponges with a dark blue color were obtained.

Characterization

The morphology of both MA sponges and PMA sponges was characterized by scanning electron microscopy (SEM, Scios 2HiVac, Thermal Fisher Scientific, Canada). The UV-Vis absorption of PEDOT:PSS solution and washing solution was measured on a UV-Vis NIR spectrometer (Cary 5000, Agilent, USA). The mechanical properties of the sponges were characterized using a dynamic mechanical analyzer (RSA-G2, TA Instruments).

Impedance measurement

Before impedance measurement, the forehead and mastoid areas (A1 and A2) were cleaned with Nuprep skin preparation gel. PMA sponge electrodes were placed on the specified locations according to the standard 10-10 EEG system, and two solid gel electrodes were placed on A1 and A2 as the reference and ground electrodes. The contact impedance spectrum was measured on the Autolab PGSTAT204 (Metrohm, Switzerland) in the range of 1 Hz to 1000 Hz and the Brain Vision Recorder software (Brain Products GmbH, Munich, Germany) at 15 Hz.

EEG recording and analysis

EEG signals were recorded from PMA sponge electrodes integrated on the Meta Quest 2 headset, fitted with a Meta Quest 2 Elite Strap (Meta, California, USA). All analysis was performed using custom MATLAB scripts and functions from EEGLAB[37].

Eye close *vs*. open comparison

EEG signals were recorded using the Brain Vision LiveAmp 32 amplifier and the Brain Vision Recorder software (Brain Products GmbH, Munich, Germany) and analyzed using custom MATLAB scripts. The experimenter recorded triggers on the Brain Vision Recorder software while giving instructions to the subject. The EEG signals were initially filtered using a bandpass filter ranging from 1.5 Hz to 50 Hz, and the alpha band was defined as 8 to 12 Hz.

VR experiment analysis

Three healthy male subjects aged 23-28 participated in the CNV recording experiment. The VR task was designed and implemented in Unity (editor version 2020.3.11f1) and was conducted using the Meta Quest 2 headset and controllers. The grand average analysis and decoding analysis were performed using signals from the Cz channel in MATLAB. The signal was preprocessed by bandpass filtering 0.1 to 1 Hz using a fourth-order Butterworth filter. Baseline correction was applied using a 100 ms window prior to Stimulus 1. Trials with an absolute sample value exceeding 50 μV were defined as artifactual and rejected from further analysis. For the decoding analysis, the EEG time samples between the two stimuli (-4.3 s before Stimulus 2 to Stimulus 2 onset) were extracted after bandpass filtering from 0.01 to 3 Hz. The extracted samples were used as features for the decoder after min-max normalization to values between 0 and 1. The decoding accuracy was computed using leave-one-out block-wise cross-validation from five blocks, using diagonal linear discriminant analysis (LDA).

RESULTS AND DISCUSSION

The design of our sponge electrode integrated VR headset for simultaneous EEG recording and VR display is illustrated in Figure 1A. The sponge electrodes were integrated onto the VR headset using a custom flexible connector array (FCA) that runs along the headset straps. Once the user wears the VR headset, the electrodes, and FCA are concealed from view. The FCA provides a soft and stable electrical connection between the electrodes and the recording system, and it is also compatible with the VR headset. In contrast, previous VR headset-integrated EEG electrodes typically rely on rigid stud connectors that have to puncture the strap to establish a connection with the recording system[17]. Moreover, the FCA enables the sponge electrodes to be distributed across various scalp locations, allowing EEG recording from multiple brain regions, including frontal, frontocentral, central, centroparietal, and occipital regions. Notably, the headset straps can apply pressure on the sponge electrodes, enabling them to deform and make better contact with the hairy scalp, thereby reducing electrode impedance. Figure 1B shows a photograph of the PMA sponges, which are 12 mm in diameter and 10 mm in height. Figure 1C shows a photograph of the FCA, comprising nine copper O-ring connectors with seamless copper traces. The entire system is fabricated on a 25 μm-thick polyethylene terephthalate (PET) substrate that can bend to conform to the headset straps, ensuring

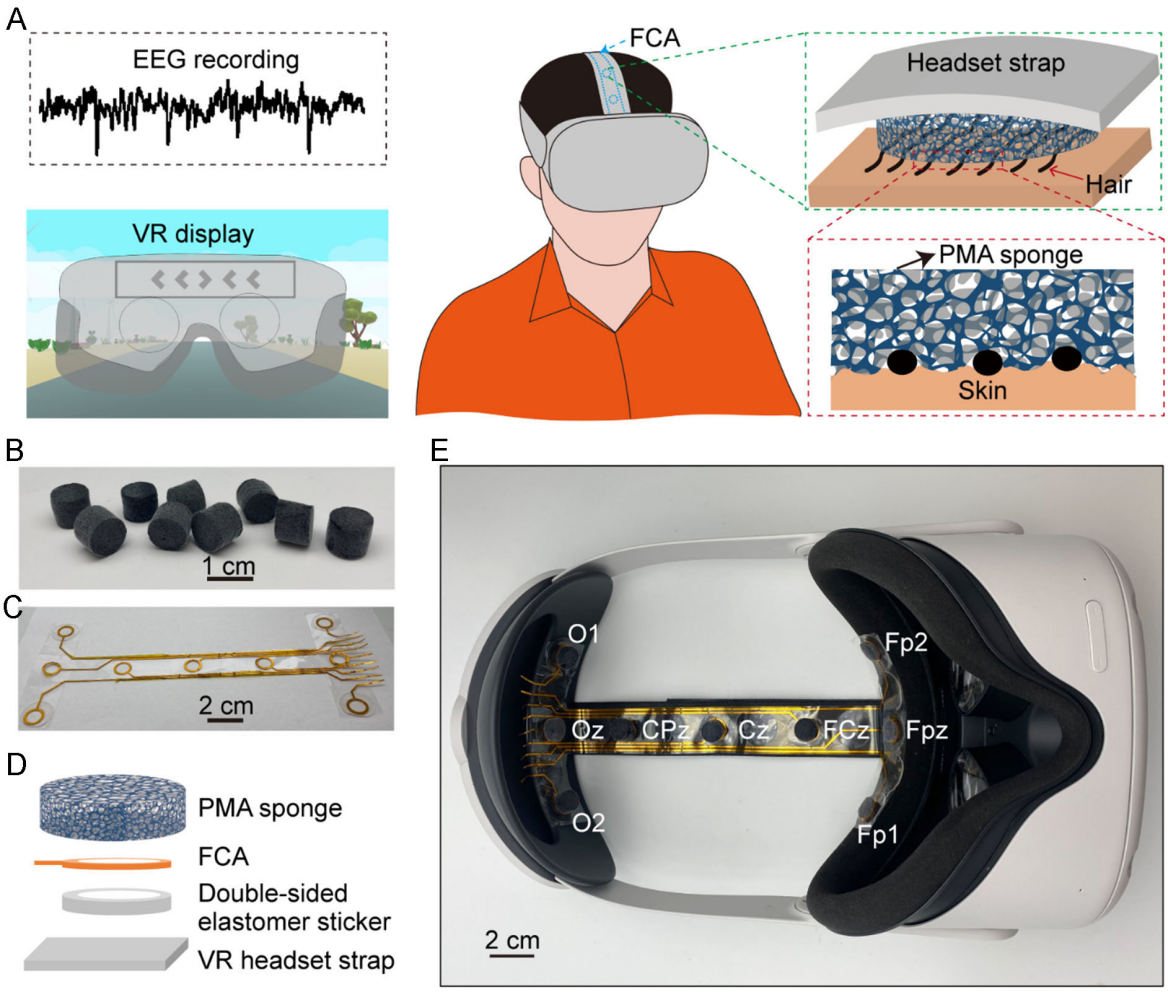

Figure 1. Design of our VR-EEG headset. (A) A schematic illustration of the PMA sponge electrodes integrated on a commercial VR headset to make good contact with the hairy scalp for EEG. The blue dash lines labeled on the VR headset strap indicate the outline of the FCA laminated on the other side of the strap; (B) A photograph of the PMA sponge electrodes; (C) A photograph of the FCA that connects all sponge electrodes to the back of the VR headset for connection to the data acquisition system; (D) An exploded view illustrating the installation of one PMA sponge on the VR headset through insertion into the open holes of the FCA, which is adhered to the strap by a double-sided elastomeric sticker; (E) The VR headset with nine PMA sponge electrodes integrated on it. EEG: electroencephalography; FCA: flexible connector array; PMA: poly (3,4-ethylenedioxythiophene) polystyrene sulfate/melamine; VR:virtual reality.

stable integration. The topside of the connectors and traces are insulated with Kapton tape to prevent direct copper-skin contact. The connector has an inner diameter of 10 mm, slightly smaller than that of the sponge, allowing it to deform and fit snugly into the connector hole for a secure connection. The FCA was fabricated using a laser cutting process [Supplementary Figure 1] , and the details of the fabrication process are provided in the supporting information. A 1 mm-thick elastomer double-sided sticker was utilized to further secure the sponge electrodes to the VR headset straps, providing stability under shear force [Figure 1D]. Figure 1E displays the VR headset equipped with nine integrated sponge electrodes, which is ready to be worn by the user for simultaneous EEG recording and VR display.

The PMA sponge was prepared using a dipping process. Figure 2A shows a schematic illustration of the fabrication process. The MA sponge cylinders were dipped in a PEDOT:PSS solution diluted with DMSO in a vacuum system to facilitate the infiltration of PEDOT:PSS solution into the pores of sponges. After removing the excess solution, the sponges were dried in an oven to evaporate the remaining solvents. The dip coating was repeated to increase the PEDOT:PSS coating and conductivity. After coating, the MA sponge changed from white to dark blue [Figure 2B], indicating successful PEDOT:PSS loading. The dried PEDOT:PSS layer is stable and non-dissolvable in water[38]. After washing the PMA sponge in saline solution ten times, no visible PEDOT absorption was detected in the UV-vis spectrum within the range of 500-800 nm[39]. However, a distinct PEDOT absorption was observed in a PEDOT:PSS solution with a low concentration of 0.02 wt.% [Supplementary Figure 2]. This result shows that the PMA sponge is inert, stable, and capable of functioning under sweaty conditions without any additional protection layer. SEM images in Figure 2C-E compare the structure of the MA sponge before and after PEDOT:PSS coating. The original MA sponge has a porous structure with a MA fiber skeleton. After the dipping process, in addition to the coating on the MA fiber skeleton, there are PEDOT:PSS flakes suspending on adjacent MA skeletons due to the evaporation of the remaining solution within the sponge [Figure 2D]. The width of the PEDOT:PSS flakes ranges in hundreds of micrometers, and the thickness of the flakes is around hundreds of nanometers. It was observed that some MA fibers with the skeletal structure exhibited fractures subsequent to the coating of PEDOT:PSS [Figure 2E]. This could potentially be attributed to the squeezing process during the fabrication of the PMA sponge. The PMA sponge is compressible [Figure 2F]. Therefore, we studied the mechanical properties of the PMA sponge and the MA sponge under different compressive strains from 30% to 90%. As shown in Figure 2G and H, the PMA sponge and the MA sponge have similar stress-strain curves at 30% and 50% strains, except for the lower Young's modulus of the PMA sponge (approximately 54.6 kPa) compared to the MA sponge (approximately 102.8 kPa) in the 0%-5% regime. We hypothesize that the partially fractured skeleton within the PMA sponge contributes to its reduced stiffness. The maximum compressive stresses of the PMA sponge at compressive strains of 70% and 90% are 33.58 kPa and 265.38 kPa, respectively, which are higher than those of the MA sponge (27.11 kPa and 83.21 kPa, respectively) due to the PEDOT:PSS flakes formed within the pores in the sponge [Figure 2D and E]. We further investigated the durability of the PMA sponge by performing consecutive loading-unloading up to a compressive strain of 50% for 20 cycles. As shown in [Supplementary Figure 3], the PMA sponge reaches similar maximum compressive stresses in every cycle, but hysteresis in stress-strain exists. The conductivity of the PMA sponge can be adjusted by modifying the dipping process and PEDOT:PSS solution concentration. The resistance of the PMA sponge prepared with one dipping is 85.62 ± 25.42 Ω, while that of the sponge prepared with two dips is 5.6 ± 2.2 Ω [Supplementary Figure 4A]. The resistance of the PMA sponge decreased from 33.2 ± 6.3 Ω to 5.6 ± 2.2 Ω as the PEDOT:PSS concentration increased from 0.39% to 0.91% [Supplementary Figure 4B]. Furthermore, the resistance of the PMA sponge can be further reduced by applying pressure, which increases the conductive path due to sponge compression [Supplementary Figure 5]. This is advantageous for the sponge electrode as it enhances the conductivity under the pressure of the VR headset strap during EEG recording.

Contact impedance plays a vital role in brain activity recordings for EEG electrodes. Therefore, we integrated the PMA sponges onto a VR headset and measured the contact impedance on both hairless and hairy sites. Using a calibrated, highly sensitive, and flexible hybrid-response pressure sensor (HRPS) developed in our group [Supplementary Figure 6][40], we have quantified that the VR headset strap can apply a pressure of 9.48-11.70 kPa on the hairless site and 10.62-12.21 kPa on the hairy site. The pressure applied by the strap can induce deformation of 25.41%-33.90% on dry sponges and 44.32%-47.71% on wet sponges. This deformation leads to a further decrease in the resistance of the sponges. The equivalent circuit model of the electrode on the hairless site is illustrated in Figure 3A. The sponge electrode is modeled as a parallel resistance (Re) and capacitance (Ce). As the electrode directly contacts the skin, the electrode-skin interface

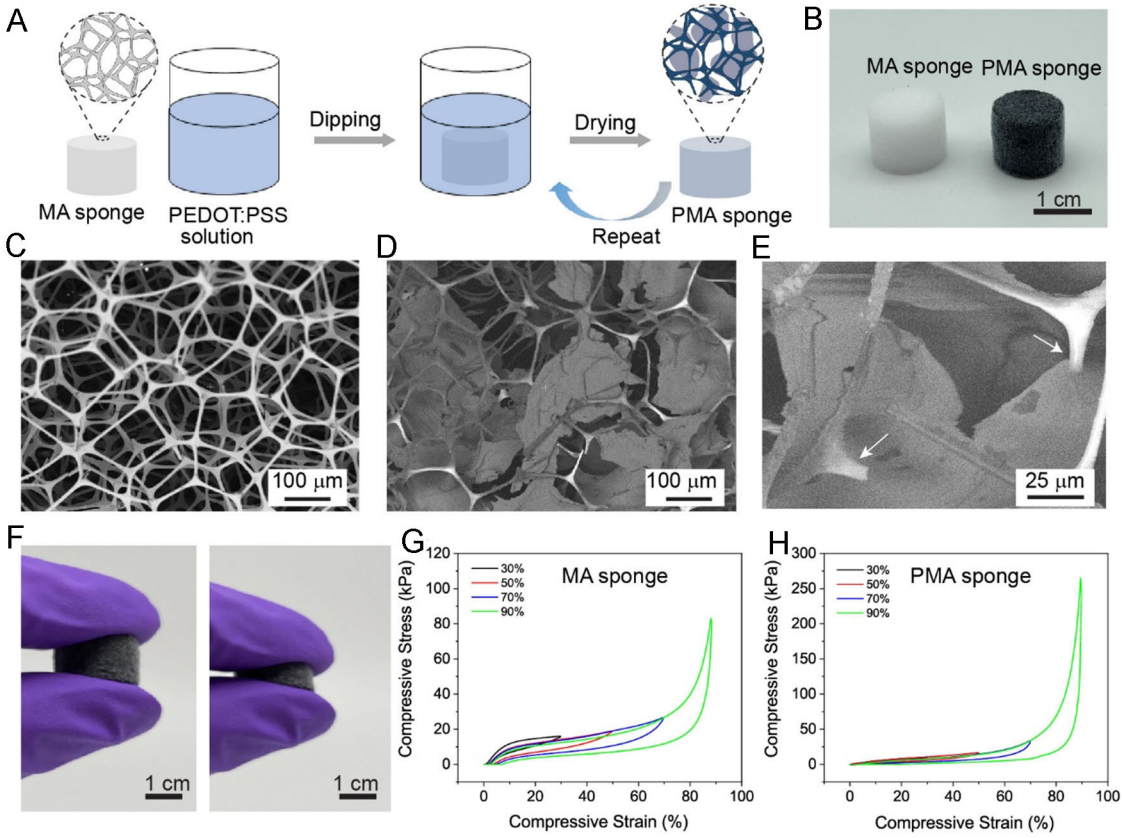

Figure 2. Fabrication, microstructure, and mechanical characterization of the PMA sponge electrode. (A) Schematic illustrations of the PMA sponge fabrication process; (B) Photographs of the MA sponge before and after PEDOT:PSS coating; (C) An SEM image of the MA sponge; (D) An SEM image of the PMA sponge with PEDOT:PSS membranes forming inside the sponge skeleton; (E) A high-resolution SEM image of the PMA sponge. The white arrows indicate that some MA ligaments ruptured during the fabrication process; (F) Photographs showing the compressibility of the PMA sponge; (G, H) Loading-unloading stress-strain curves of the MA and PMA sponges under maximum compressive strains varying from 30% to 90%. MA: melamine; PMA: poly (3,4-ethylenedioxythiophene) polystyrene sulfate/melamine; PEDOT: PSS: poly(3,4-ethylenedioxythiophene) polystyrene sulfonate; SEM: scanning electron microscopy.

is modeled as a contact resistance (Rc) and capacitance (Cc), which is determined by the gap between the electrode and the skin. The epidermis and dermis are modeled as a resistor-capacitor (RC) circuit (R_{Ep}, C_{Ep}) and a resistor (Rd), respectively. The softness of the sponge electrode allows it to form good contact with the skin and minimize the gap, leading to a small Rc and large Cc. We measured the contact impedance of the sponge electrodes at the Fp1 and Fp2 locations while wearing the VR headset across three subjects. The results are plotted in Figure 3B, with the error bars indicating the standard deviation. The full frequency spectrum collected by the electrochemical workstation (Autolab PGSTAT204) shows that the sponge electrode has an average specific impedance of 12.73 ± 4.67 kΩ·cm² at 10 Hz, while that for a solid gel electrode (Kendall ECG electrodes) is 3.79 ± 2.53 kΩ·cm². The variation in impedance is attributed to the diverse skin conditions among the subjects. Given the chemical stability of our sponge electrodes, we further investigated their impedance under wet conditions on the same subject. The wet sponge was prepared by adding several drops of deionized water to the sponge and squeezing out the excess liquid. The specific contact impedance of the wet sponge obtained by the Brain Vision Recorder software is 6.41 ± 0.58 kΩ·cm² at 15 Hz, which is three times lower than that of the dry electrode (19.40 ± 3.60 kΩ·cm² at 15 Hz) [Figure 3C]. One possible reason for the reduced impedance under wet conditions is that the wetting

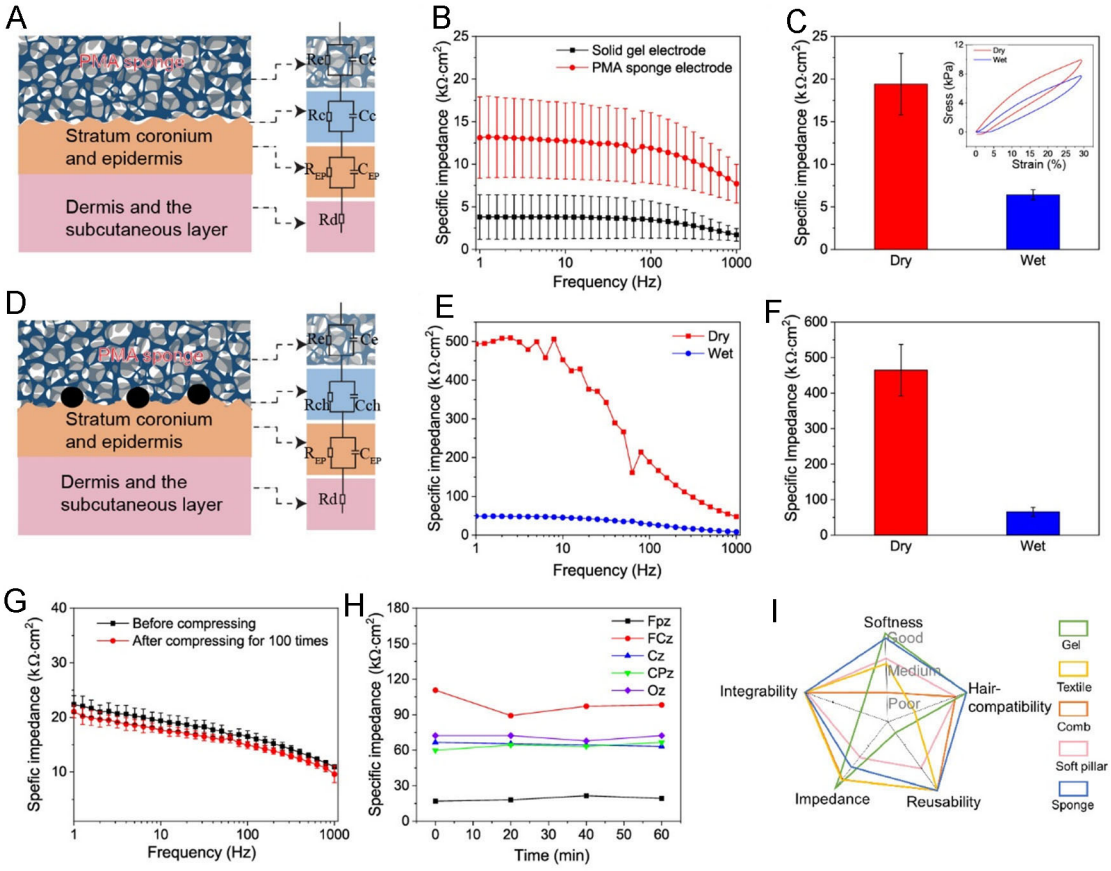

Figure 3. Contact impedance of the sponge electrode on hairless skin (A-C) and hairy skin (D-F). (A) Cross-sectional schematic and equivalent circuit model of the sponge electrode on hairless skin; (B) Electrode-skin impedance spectrum of the sponge electrode and solid gel electrode on a total of nine hairless sites of three different subjects. The markers are average values, and the error bars indicate the standard deviation; (C) A comparison of the contact impedance between the dry and wet sponge electrodes on hairless skin (n = 6). The inset plots the loading-unloading stress- strain curves of dry (black) and wet (red) sponges; (D) Cross-sectional schematic and equivalent circuit model of the sponge electrode on hairy skin; (E) Electrode-skin impedance spectrum of the sponge electrode and solid gel electrode on the hairy scalp; (F) A comparison of the contact impedance between the dry and wet sponge electrodes on the hairy sites (n = 6); (G) Electrode-skin contact impedance spectrum of the sponge electrode before (black) and after (red) being compressed 100 times (three measurements at each frequency); (H) The contact impedance of the sponge electrodes on different locations is stable after 60 min of continuous wear; (I) A radar chart that compares the sponge electrodes with other EEG electrodes in the literature based on the impedance, softness, hair compatibility, and reusability criteria. Grading is based on the following criteria. Impedance lower than 10 kΩ·cm^2 is good, 10 kΩ·cm^2-100 kΩ·cm^2 is medium, and higher than 100 kΩ·cm^2 is poor. Softness with Young's modulus lower than 50 kPa is good, 50 kPa-1 MPa is medium, and higher than 1 MPa is poor. Hair compatibility, if the electrode cannot deform to contact the hairy scalp, it is considered poor; if the electrode can deform to reach the hairy scalp but has medium impedance, it is defined as medium; if the electrode can form very good contact with the hairy scalp with good impedance, it is considered high. Reusability: if the electrode can be reused without being destroyed after use, it is considered good; otherwise, it is considered poor. EEG: electroencephalography.

process makes the sponge softer, leading to a change of Young's modulus from approximately 54.6 kPa to 30.0 kPa [inset, Figure 3C]. This change in modulus allows the sponge to deform more easily when pressed by the headset strap, resulting in better electrode-skin contact and an increase in Cc. Another possible reason is that the stratum coronium has an improved conductivity when wet[41], contributing to a lower impedance with a reduced $R_{Ep.}$

We further studied the contact impedance of sponge electrodes on the hairy scalp by integrating two sponges on the O1 and O2 locations of the VR headset. The equivalent circuit model of the sponge on the

hairy site is similar to that on the hairless site, except that the hair creates an additional barrier between the electrode and the skin. The electrode-hairy skin interface is modeled as an RC circuit of Rch and Cch, where Rch and Cch are the contact resistance and the contact capacitance, respectively [Figure 3D]. The full frequency spectrum shows that the dry sponge electrodes have a high specific impedance of 452.71 kΩ·cm² at 10 Hz due to the separating effect of the hair. By contrast, when wet, the specific impedance of the sponge decreased to 45.50 kΩ·cm² at 10 Hz, which is approximately ten times lower than that of the dry sponge [Figure 3E]. Impedance measurement by the Brain Vision Recorder software showed that the dry sponge on the hairy site has a specific impedance of 464.71 ± 72.24 kΩ·cm² at 15 Hz, while the wet sponge has a much lower specific impedance of 65.54 ± 12.67kΩ·cm² at 15 Hz [Figure 3F]. These results further highlight the importance of the softness of sponges in establishing a good interface with the hairy scalp and reducing impedance. In addition, since no skin preparation was done on the hairy site, the stratum corneum on the hairy scalp is thicker, resulting in a more significant increase in conductivity compared to the forehead.

The mechanical stability of the sponge under repeated compression is essential for reusability. As shown in Figure 3G, the specific impedance of the sponge remains unchanged after 100 cycles of squeezing at 50% compressive strain, demonstrating that the sponge electrodes can be used multiple times with the VR headset. The electrochemical stability of the electrode over a prolonged period is crucial for long-term EEG signal recording. Therefore, we measured the stability of electrode impedance in different locations for 60 minutes. The contact impedance varied depending on the location of the electrode, with the dry sponge on the forehead exhibiting lower impedance compared to the wet sponges on the hairy scalp [Figure 3H]. Most of the electrodes exhibited stable impedance over time. Furthermore, we investigated the reusability of the PMA sponge. As shown in Supplementary Figure 7, the electrode exhibited similar impedance after putting on and taking off the VR headset ten times, indicating that our sponge electrode can be used for at least ten uses. Finally, we compared our sponge electrodes with other types of electrodes in the literature, including wet gel, textile, comb electrodes, and soft pillar electrodes. We can see that our sponge electrode outperforms those electrodes with softness, low impedance, good compatibility with hair, ease of integrability, and reusability [Figure 3I, Table 1]. In comparison to other sponge electrodes [Table 1][17,29,42], our PMA sponges were simply but reliably integrated onto the VR headset through an ultrathin FCA, making the whole system easy to assemble and also soft and comfortable to wear.

Next, we studied the capability of the sponge electrodes to record EEG signals during eye-close and eye-open conditions, using four participants in our study. The purpose of this experiment is to demonstrate that sponge electrodes can successfully record increased alpha rhythm, which is a characteristic of EEG that is present during the absence of visual stimuli, such as the eyes being closed. The sponge electrodes were integrated onto the VR headset using a flexible FCA at Fp2 as a hairless site and Cz and Oz as hairy sites [Figure 4A]. The end of the FCA can be directly connected to the EEG data acquisition system without requiring additional fixation [Figure 4B]. As shown in Figure 4C, the filtered EEG signals from Cz and Oz demonstrated a clear increase in amplitude in the alpha band (8-12 Hz) during the eye-close period compared to the eye-open period, resulting in increased power. Time-frequency analysis and power spectra density (PSD) results confirmed this increase in alpha power in the range of 8-12 Hz during the eye-closed period compared to the eye-open period [Figure 4D and E]. Thus, the EEG data recorded with the sponge electrode exhibited the characteristic feature of increased alpha oscillation power during the absence of visual stimulation[43]. The stable integration of the sponge electrodes on the VR headset enables consistent EEG recording over a typical VR session of 60 minutes [Supplementary Figure 8], which is sufficient considering that typical VR applications do not exceed this duration to avoid issues such as VR cybersickness and discomfort[12]. We also compared the performance of our sponge electrodes with commercial electrodes on both hairless and hairy sites. For hairless sites, we attached a solid gel electrode at

Table 1. Summary of the performance of different types of hairy-compatible EEG electrodes

Materials	Fabrication	Softness	Hair compatibility	Specific Impedance ($k\Omega \cdot cm^2$)	Connection	Ref.
PMA sponge	Dip coating	Yes	Yes	19.40 ± 3.60 (15 Hz, forehead) 65.54 ± 12.67 (15 Hz, hairy site)	FCA	This work
Gelatin gel	Chemical polymerization	Yes	Yes	5.46 ± 0.76 (10 Hz, hairy site)	Stud	Wang *et al.*[22]
PEDOT hydrogel	Chemical polymerization	Yes	Yes	20.7 (10 Hz, hairy site)	Stud	Hsieh *et al.*[9]
PEDOT:PSS-coated PDMS pillars	Replica and coating	Yes	Yes	--	--	Zhang *et al.*[28]
Au-coated silicon pin	Microfabrication and thermal deposition	Yes	Yes	7.5 (10 Hz, hairy site)	--	Wang *et al.*[23]
Cellulose sponge	--	No	Yes	1171.3 (forehead); 1089-1727.9 (hairy site)	Stud	Ko *et al.*[42]
Conductive fabric and metal-coated sponge	--	Yes	No	18.1-28.3 (15 Hz, forehead); 53.1-91.5 (15 Hz, hairy site)	Stud	Kuang *et al.*[18]
Ag NW/MA sponge	Dip coating	Yes	Yes	0.6-1.2 (30 Hz, hairy site)	Silver wire	Lin *et al.*[29]

FCA: flexible connector array; MA: melamine; PMA: poly (3,4-ethylenedioxythiophene) polystyrene sulfate/melamine; PEDOT:PSS: poly(3,4-ethylenedioxythiophene) polystyrene sulfonate

the Fp1 location, which had similar skin conditions to the neighboring Fp2 [Supplementary Figure 9A]. Our sponge electrode demonstrated similar EEG features to the solid gel electrode, with a Pearson's correlation coefficient (r) of 0.977 between the EEG signals recorded by the two electrodes [Figure 4F]. On hairy sites, our sponge electrode performed comparably to a commercial comb electrode located adjacent to it near Cz [Supplementary Figure 9B], with a Pearson's correlation coefficient (r) of 0.860 [Figure 4G]. It is worth noting that the sponge electrode is compatible, soft, and skin-friendly, not causing any skin irritation and not leaving visible markings after wearing for 1 hour, whereas the comb electrode is stiff and uncomfortable, leaving noticeable marks on the skin [Supplementary Figure 10]. The ease of setup, high stability, and user-friendliness of our sponge-electrode-integrated VR headset makes it a promising system for simultaneous EEG recording and VR interaction.

Finally, we evaluated the performance of our sponge electrode in a VR-BCI system. To this end, we designed a CNV task in a custom first-person perspective VR game for the "Go/No-Go" classification. The electrode was placed on Cz, located over the central region of the cerebral cortex [Figure 5A], which is a typical location of interest for detecting CNV potentials. CNV is a well-established slow cortical EEG potential associated with anticipation and attention generated from sources in the prefrontal and central regions of the cerebral cortex[44-46]. Our VR game was designed to resemble decision-making while driving, which is a commonly used scenario and application for CNV-based BCIs [Figure 5B, Movie S1][47-49]. The subject was instructed to remember the direction of the middle symbol of the Flanker task (Stimulus 1) [Figure 5C][50] and respond exactly 4.3 seconds later (as guided by the countdown on display) by pressing a button on the VR controller the moment the diverging sign (Stimulus 2) appeared when the Stimulus 1 was a "Go". If Stimulus 1 was a "No-Go", the subject was instructed to ignore Stimulus 2. The input was only accepted within a 300 ms window after Stimulus 2, and the response time of the subject was displayed as feedback during the "Go" trials to keep the subject alert to Stimulus 2 [Figure 5B]. Positive visual feedback in the form of a gem object and an increasing score was delivered if the response of the subject was correct

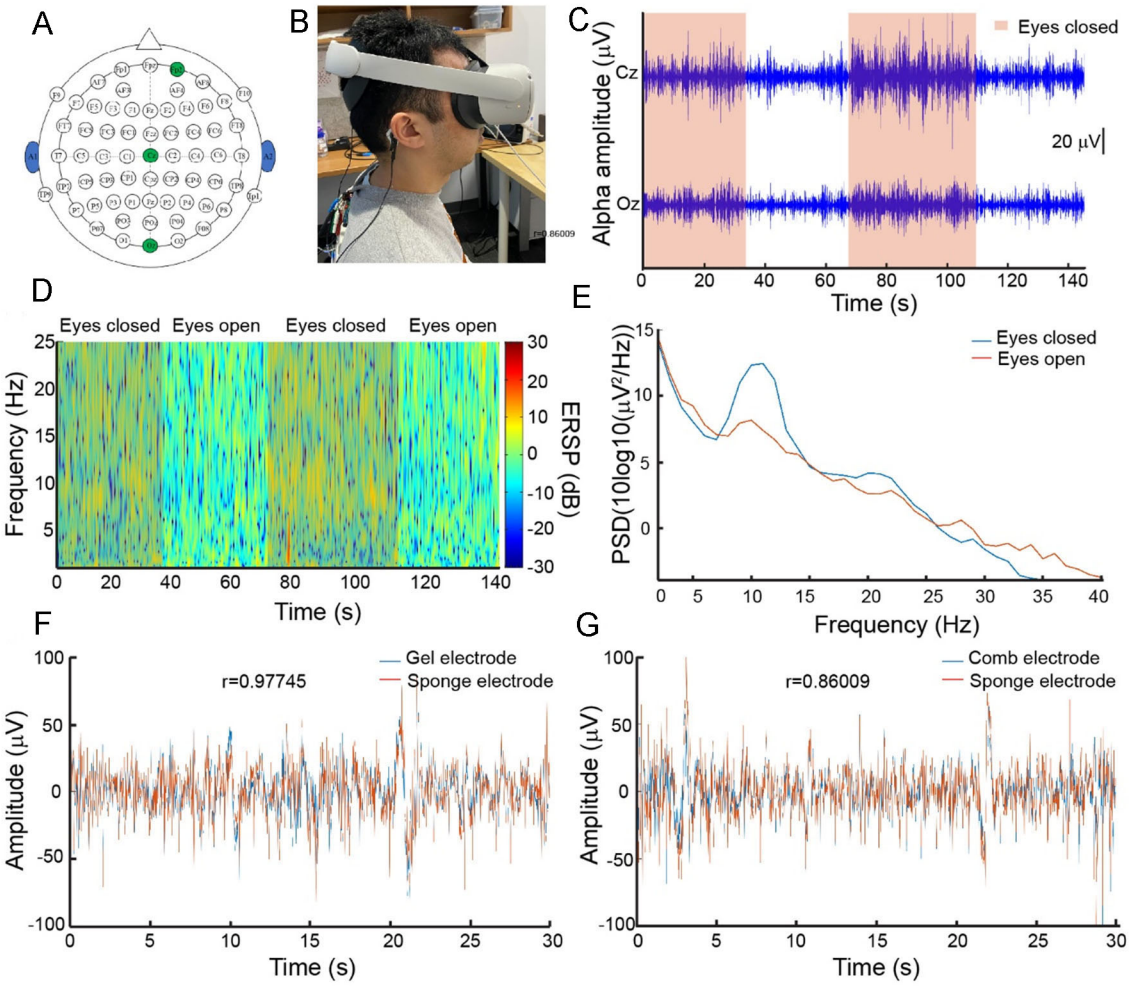

Figure 4. PMA sponge electrodes integrated on a VR headset for EEG recording; (A) Placement of sponge electrodes on a VR headset, with Fp2 at a hairless site and Cz and Oz at hairy sites; (B) The complete setup for EEG recording in which commercial cables are clipped on the FCA terminals; (C) Alpha bandpass filtered EEG signals (8-12 Hz) captured during eye-close and eye-open periods from one subject, with similar results for three other participants; (D) Time-frequency analysis of the EEG signals recorded at Oz, showing event-related spectral perturbation (ERSP) as a ratio of average amplitudes in the experimental condition (eyes-close or eye-open) to baseline epoch (taken from the start of the recording before subject instructions were given). In (C) and (D), shaded areas indicate eye-closed periods; (E) PSD of the EEG signals recorded at Oz during eye-close (blue) and eye-open (red) conditions; (F) Comparison of the EEG signals recorded by the sponge electrode and the solid gel electrode at comparable locations (Fp2 and Fp1, respectively) after bandpass filtering (1.5-50 Hz); (G) Comparison of EEG signals recorded by the sponge electrode (Cz) and a commercial comb electrode (OpenBCI) located adjacent to it. EEG: electroencephalography; PMA: poly (3,4-ethylenedioxythiophene) polystyrene sulfate/melamine; VR: virtual reality.

(i.e., if the button was pressed within the input window for a "Go" trial or if the button was not pressed for a "No-Go" trial).

In the VR-BCI experiment, three subjects completed five blocks of the VR task while EEG was simultaneously recorded using the sponge electrode. Each block consisted of 6 "Go" and 6 "No-Go" trials. Grand average analysis of the EEG signals showed that a negative potential slope was developed between the two stimuli only for "Go" trials [Figure 5D], which is consistent with the result in previous reports[46]. Leave-one-out block-wise cross-validation was performed, resulting in a cross-validated area under the receiver operating characteristic curve (AUC) of 0.66 ± 0.07 for the three subjects [Figure 5E].

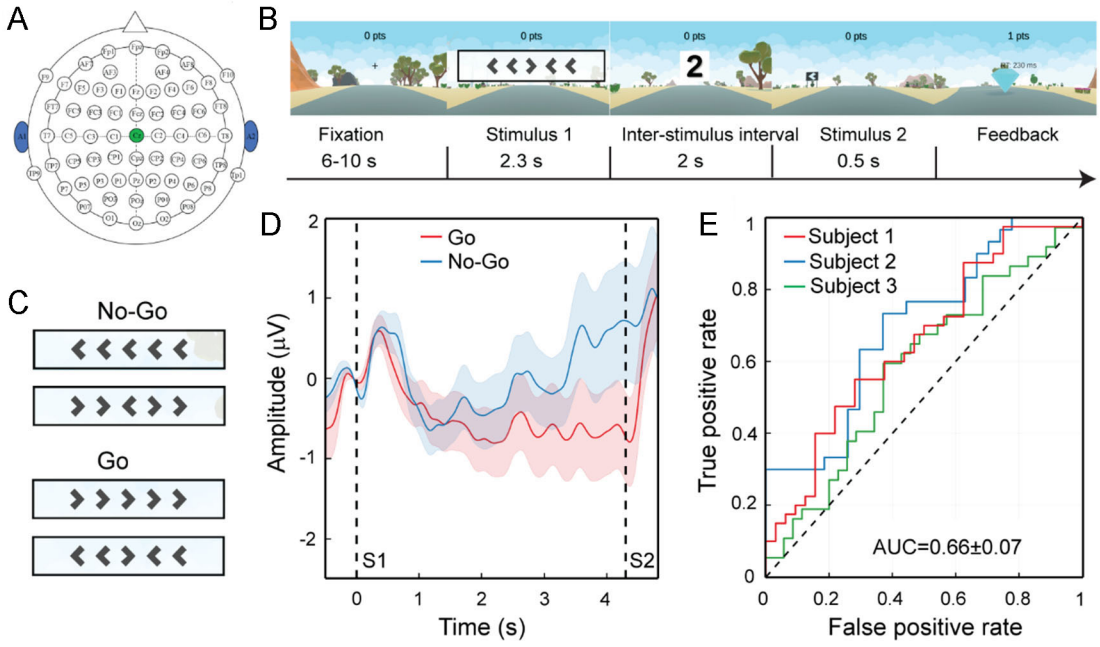

Figure 5. Demonstration of the sponge-electrode-integrated VR-EEG headset used for BCI. (A) Placement of the electrodes during CNV recording; (B) CNV task structure. Subjects participated in five blocks of the VR task, with each block consisting of 12 trials. Each trial consisted of a 6-8 second inter-trial interval, followed by the display of stimulus 1 for 2.3 seconds, an inter-stimulus period of 2 seconds, and the display of stimulus 2 for 0.5 seconds, which ended with visual feedback; (C) Stimulus 1 was delivered in the form of a Flanker task, with subjects being instructed to keep the middle symbol in mind and respond after stimulus 2 appeared. The subjects were instructed to press the button if seeing ">" in the middle symbol and not to press it if the middle symbol was displayed to be "<"; (D) CNV grand average signal of Go and No-Go trials from the three subjects. The blue and red shaded lines represent the standard error mean, while S1 and S2 denote the onsets of Stimulus 1 and 2; (E) Receiver operating characteristic (ROC) curves of the CNV decoder used in the CNV-VR experiment.BCI: brain-computer interfaces; CNV: contingent negative variation; . EEG: electroencephalography; VR:virtual reality.

CONCLUSIONS

In this paper, we developed soft and conductive PMA sponge electrodes that can be integrated with a commercial VR headset for simultaneous EEG recording and immersive VR stimulation. The sponge electrodes can form sufficient contact with both hairless and hairy scalps for high-quality EEG recordings. In addition, the sponge electrode is compressible and can maintain a stable contact impedance with the skin after 100 cycles of compression, which enhances the durability and longevity of the electrode. Our sponge-electrode-integrated VR headset allowed for stable measurement of EEG features, such as alpha rhythms, for 60 minutes. Furthermore, we have demonstrated that our electrodes are capable of recording VR-evoked CNV potentials. Our VR-EEG system is easy to set up, reliable for EEG recordings during VR interaction, user-friendly, customizable, and has the potential for use in various applications requiring simultaneous EEG recording and VR interaction. In the future, through custom-designed VR headset straps and FCA, more sponge electrodes can be placed strategically for EEG recordings from desirable brain regions depending on the application, such as recording other event-related potentials, sensorimotor rhythms, *etc.*, for the purposes of emotion recognition or workload evaluation. Moreover, VR headsets that can conform to the scalp and provide consistent pressure could significantly enhance the quality of recorded EEG during even longer periods of time.

DECLARATIONS

Authors' contributions

Conceptualization, electrode preparation, methodology, data acquisition, analysis, and interpretation, writing original draft: Li H

Methodology, data acquisition, software and data analysis, manuscript revising: Shin H, Zhang M, Huh H, Riveira N, Kwon G

Electrode preparation, data acquisition, manuscript revising: Yu A, Gangopadahyay S, Peng J, Rao Y, Li Z, Kim S

Supervision, funding acquisition, and manuscript revision: Sentis L

Project discussion, supervision, and manuscript revision: Millán JdR

Conceptualization, funding acquisition, project administration, resources, supervision and writing, review, and editing: Lu N

Availability of data and materials

Not applicable.

Financial support and sponsorship

NL acknowledges the support from the U.S. Army Research Office under Cooperative Agreement (W911NF-19-2-0333). LS acknowledges the support from the U.S. National Science Foundation GCR Grant (2219236) and the U.S. Army Research Laboratory under Cooperative Agreement (W911NF2120163). The views and conclusions contained in this review are those of the authors and should not be interpreted as representing the official policies, either expressed or implied, of the U.S. Army Research Office, U.S. National Science Foundation, U.S. Army Research Laboratory, or the U.S. government.

Conflicts of interest

All authors declared that there are no conflicts of interest.

Ethical approval and consent to participate

The study was conducted in accordance with the ethical guidelines and principles set forth by the Internal Review Board (IRB) of the University of Texas at Austin under approval number STUDY00004005. All participants were informed about the experimental procedure and signed the informed consent forms prior to participation.

Consent for publication

Not applicable.

REFERENCES

1. Yuan H, Li Y, Yang J, et al. State of the art of non-invasive electrode materials for brain-computer interface. *Micromachines* 2021;12:1521. DOI PubMed PMC
2. Yang L, Liu Q, Zhang Z, Gan L, Zhang Y, Wu J. Materials for dry electrodes for the electroencephalography: advances, challenges, perspectives. *Adv Mater Technol* 2022;7:2100612. DOI
3. Lopez-Gordo MA, Sanchez-Morillo D, Pelayo Valle F. Dry EEG electrodes. *Sensors* 2014;14:12847-70. DOI PubMed PMC
4. Campbell IG. EEG recording and analysis for sleep research. *Curr Protoc Neurosci* 2009;Chapter 10:Unit10.2. DOI PubMed PMC
5. Noachtar S, Rémi J. The role of EEG in epilepsy: a critical review. *Epilepsy Behav* 2009;15:22-33. DOI PubMed
6. Cervera MA, Soekadar SR, Ushiba J, et al. Brain-computer interfaces for post-stroke motor rehabilitation: a meta-analysis. *Ann Clin Transl Neurol* 2018;5:651-63. DOI PubMed PMC
7. Wolpaw JR, Millán JdR, Ramsey NF. Chapter 2 - Brain-computer interfaces: definitions and principles. *Handb Clin Neurol* 2020;168:15-23. DOI

8. Orban M, Elsamanty M, Guo K, Zhang S, Yang H. A review of brain activity and EEG-based brain-computer interfaces for rehabilitation application. *Bioengineering* 2022;9:768. DOI PubMed PMC
9. Hsieh JC, Alawieh H, Li Y, et al. A highly stable electrode with low electrode-skin impedance for wearable brain-computer interface. *Biosens Bioelectron* 2022;218:114756. DOI
10. Miskowiak KW, Jespersen AE, Kessing LV, et al. Cognition assessment in virtual reality: validity and feasibility of a novel virtual reality test for real-life cognitive functions in mood disorders and psychosis spectrum disorders. *J Psychiatr Res* 2021;145:182-9. DOI
11. Maggio MG, Latella D, Maresca G, et al. Virtual reality and cognitive rehabilitation in people with stroke: an overview. *J Neurosci Nurs* 2019;51:101-5. DOI
12. Tashjian VC, Mosadeghi S, Howard AR, et al. Virtual reality for management of pain in hospitalized patients: results of a controlled trial. *JMIR Ment Health* 2017;4:e9. DOI PubMed PMC
13. Coogan CG, He B. Brain-computer interface control in a virtual reality environment and applications for the internet of things. *IEEE Access* 2018;6:10840-9. DOI PubMed PMC
14. Cipresso P, Giglioli IAC, Raya MA, Riva G. The past, present, and future of virtual and augmented reality research: a network and cluster analysis of the literature. *Front Psychol* 2018;9:2086. DOI
15. Krokos E, Varshney A. Quantifying VR cybersickness using EEG. *Virtual Reality* 2022;26:77-89. DOI
16. Suhaimi NS, Mountstephens J, Teo J. A dataset for emotion recognition using virtual reality and EEG (DER-VREEG): emotional state classification using low-cost wearable VR-EEG headsets. *Big Data Cogn Comput* 2022;6:16. DOI
17. Zhang Y, Zhang L, Hua H, et al. Relaxation degree analysis using frontal electroencephalogram under virtual reality relaxation scenes. *Front Neurosci* 2021;15:719869. DOI PubMed PMC
18. Kuang F, Shu L, Hua H, et al. Cross-subject and cross-device wearable EEG emotion recognition using frontal EEG under virtual reality scenes. In: IEEE International Conference on Bioinformatics and Biomedicine (BIBM); Houston, TX, USA; 2021. p. 3630-7. DOI
19. Li G, Wu J, Xia Y, He Q, Jin H. Review of semi-dry electrodes for EEG recording. *J Neural Eng* 2020;17:051004. DOI PubMed
20. Goulart LA, Guaraldo TT, Lanza MRV. A novel electrochemical sensor based on printex L6 carbon black carrying CuO/Cu_2O nanoparticles for propylparaben determination. *Electroanalysis* 2018;30:2967-76. DOI
21. Luo J, Sun C, Chang B, et al. MXene-enabled self-adaptive hydrogel interface for active electroencephalogram interactions. *ACS Nano* 2022;16:19373-84. DOI
22. Wang C, Wang H, Wang B, et al. On-skin paintable biogel for long-term high-fidelity electroencephalogram recording. *Sci Adv* 2022;8:eabo1396. DOI PubMed PMC
23. Wang R, Jiang X, Wang W, Li Z. A microneedle electrode array on flexible substrate for long-term EEG monitoring. *Sens Actuators B Chem* 2017;244:750-8. DOI
24. Song Y, Li P, Li M, et al. Fabrication of chitosan/Au-TiO_2 nanotube-based dry electrodes for electroencephalography recording. *Mater Sci Eng C Mater Biol Appl* 2017;79:740-7. DOI PubMed
25. Aghazadeh H, Yazdi MK, Kolahi A, et al. Synthesis, characterization and performance enhancement of dry polyaniline-coated neuroelectrodes for electroencephalography measurement. *Curr Appl Phys* 2021;27:43-50. DOI
26. Liu J, Liu X, He E, et al. A novel dry-contact electrode for measuring electroencephalography signals. *Sens Actuator A Phys* 2019;294:73-80. DOI
27. Arai M, Kudo Y, Miki N. Polymer-based candle-shaped microneedle electrodes for electroencephalography on hairy skin. *Jpn J Appl Phys* 2016;55:06GP16. DOI
28. Zhang L, Kumar KS, He H, et al. Fully organic compliant dry electrodes self-adhesive to skin for long-term motion-robust epidermal biopotential monitoring. *Nat Commun* 2020;11:4683. DOI PubMed PMC
29. Lin S, Liu J, Li W, et al. A flexible, robust, and gel-free electroencephalogram electrode for noninvasive brain-computer interfaces. *Nano Lett* 2019;19:6853-61. DOI
30. Baek HJ, Lee HJ, Lim YG, Park KS. Conductive polymer foam surface improves the performance of a capacitive EEG electrode. *IEEE Trans Biomed Eng* 2012;59:3422-31. DOI PubMed
31. Shu L, Xu T, Xu X. Multilayer sweat-absorbable textile electrode for EEG measurement in forehead site. *IEEE Sensors J* 2019;19:5995-6005. DOI
32. Liu J, Lin S, Li W, et al. Ten-hour stable noninvasive brain-computer interface realized by semidry hydrogel-based electrodes. *Research* 2022;2022:9830457. DOI PubMed PMC
33. Kayser LV, Lipomi DJ. Stretchable conductive polymers and composites based on PEDOT and PEDOT:PSS. *Adv Mater* 2019;31:1806133. DOI PubMed PMC
34. Ding Y, Yang J, Tolle CR, Zhu Z. Flexible and compressible PEDOT:PSS@melamine conductive sponge prepared via one-step dip coating as piezoresistive pressure sensor for human motion detection. *ACS Appl Mater Interfaces* 2018;10:16077-86. DOI
35. Cui XT, Zhou DD. Poly (3,4-ethylenedioxythiophene) for chronic neural stimulation. *IEEE Trans Neural Syst Rehabil Eng* 2007;15:502-8. DOI PubMed
36. Zucca A, Cipriani C, Sudha, et al. Tattoo conductive polymer nanosheets for skin-contact applications. *Adv Healthc Mater* 2015;4:983-90. DOI
37. Delorme A, Makeig S. EEGLAB: an open source toolbox for analysis of single-trial EEG dynamics including independent component

analysis. *J Neurosci Methods* 2004;134:9-21. DOI PubMed

38. Beccatelli M, Villani M, Gentile F, et al. All-polymeric pressure sensors based on PEDOT:PSS-modified polyurethane foam. *ACS Appl Polym Mater* 2021;3:1563-72. DOI
39. Pacios R, Marcilla R, Pozo-Gonzalo C, et al. Combined electrochromic and plasmonic optical responses in conducting polymer/metal nanoparticle films. *J Nanosci Nanotechnol* 2007;7:2938-41. DOI
40. Ha KH, Zhang W, Jang HW, et al. Highly sensitive capacitive pressure sensors over a wide pressure range enabled by the hybrid responses of a highly porous nanocomposite. *Adv Mater* 2021;33:2103320. DOI
41. Ferrari LM, Ismailov U, Badier J, Greco F, Ismailova E. Conducting polymer tattoo electrodes in clinical electro- and magneto-encephalography. *npj Flex Electron* 2020;4:4. DOI
42. Ko LW, Chang Y, Wu PL, Lu YC, Yeh CL, Chen YJ. Novel moisture retention sponge electrodes for developing a wireless EEG SSVEP-based BCI system. In: International Automatic Control Conference (CACS), Taoyuan, Taiwan, 2018, pp. 1-6. DOI
43. Compston A. The Berger rhythm: potential changes from the occipital lobes in man, by E. D. Adrian and B. H. C. Matthew (From the Physiological Laboratory, Cambridge). Brain 1934: 57; 355-385. *Brain* 2010;133:3-6. DOI
44. Walter WG, Cooper R, Aldridge VJ, Mccallum WC, Winter AL. Contingent negative variation: an electric sign of sensorimotor association and expectancy in the human brain. *Nature* 1964;203:380-4. DOI PubMed
45. Nagai Y, Critchley HD, Featherstone E, Fenwick PBC, Trimble MR, Dolan RJ. Brain activity relating to the contingent negative variation: an fMRI investigation. *Neuroimage* 2004;21:1232-41. DOI
46. Garipelli G, Chavarriaga R, Millán JdR. Single trial analysis of slow cortical potentials: a study on anticipation related potentials. *J Neural Eng* 2013;10:036014. DOI
47. Guo Z, Tan X, Pan Y, et al. Contingent negative variation during a modified cueing task in simulated driving. *PLoS One* 2019;14:e0224966. DOI PubMed PMC
48. Khaliliardali Z, Chavarriaga R, Zhang H, Gheorghe LA, Perdikis S, Millán JdR. Real-time detection of driver's movement intention in response to traffic lights. *bioRxiv* 2019:443390. DOI
49. Khaliliardali Z, Chavarriaga R, Gheorghe LA, Millán JdR. Action prediction based on anticipatory brain potentials during simulated driving. *J Neural Eng* 2015;12:066006. DOI PubMed
50. Hübner R, Töbel L. Conflict resolution in the Eriksen flanker task: similarities and differences to the Simon task. *PLoS One* 2019;14:e0214203. DOI PubMed PMC